Quaternion-Based Self-Attentive Long Short-term User Preference Encoding for Recommendation

Thanh Tran*
Worcester Polytechnic Institute
tdtran@wpi.edu

Di You*
Worcester Polytechnic Institute
dyou@wpi.edu

Kyumin Lee
Worcester Polytechnic Institute
kmlee@wpi.edu

ABSTRACT

Quaternion space has brought several benefits over the traditional Euclidean space: Quaternions (i) consist of a real and three imaginary components, encouraging richer representations; (ii) utilize Hamilton product which better encodes the inter-latent interactions across multiple Quaternion components; and (iii) result in a model with smaller degrees of freedom and less prone to overfitting. Unfortunately, most of the current recommender systems rely on real-valued representations in Euclidean space to model either user's long-term or short-term interests. In this paper, we fully utilize Quaternion space to model both user's long-term and short-term preferences. We first propose a QUaternion-based self-Attentive Long term user Encoding (*QUALE*) to study the user's long-term intents. Then, we propose a QUaternion-based self-Attentive Short term user Encoding (*QUASE*) to learn the user's short-term interests. To enhance our models' capability, we propose to fuse *QUALE* and *QUASE* into one model, namely *QUALSE*, by using a Quaternion-based gating mechanism. We further develop Quaternion-based Adversarial learning along with the Bayesian Personalized Ranking (*QABPR*) to improve our model's robustness. Extensive experiments on six real-world datasets show that our fused QUALSE model outperformed 11 state-of-the-art baselines, improving 8.43% at *HIT@1* and 10.27% at *NDCG@1* on average compared with the best baseline.

CCS CONCEPTS

• **Information systems → Recommender systems**.

KEYWORDS

Long-term and short-term user preferences; Quaternion-based recommenders; Quaternion-based attention; adversarial training.

ACM Reference Format:
Thanh Tran, Di You, and Kyumin Lee. 2020. Quaternion-Based Self-Attentive Long Short-term User Preference Encoding for Recommendation. In *Proceedings of the 29th ACM International Conference on Information and Knowledge Management (CIKM '20), October 19–23, 2020, Virtual Event, Ireland*. ACM, New York, NY, USA, 10 pages. https://doi.org/10.1145/3340531.3411926

*Denotes equal contribution.

CIKM '20, October 19–23, 2020, Virtual Event, Ireland

ACM ISBN 978-1-4503-6859-9/20/10…$15.00
https://doi.org/10.1145/3340531.3411926

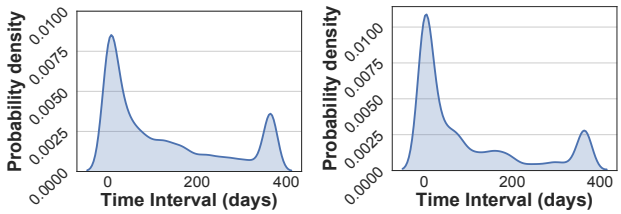

(a) Video Games (b) Toys and Games

Figure 1: Density distribution of item-item similarity scores on Amazon *Video Games*, and *Toys and Games* datasets.

1 INTRODUCTION

Recommender Systems [31] have become the heart of many online applications such as e-commerce, music/video streaming services, social media, *etc.* Recommender systems proactively helped (i) users to explore new/unseen items, (ii) potentially the users stay longer on the applications, and (iii) companies increase their revenue.

Matrix Factorization techniques [10, 13, 18] extracted features of users and items to compute their similarity. Recently, deep neural network boosted performance of a recommender system by providing non-linearity which helped modeling complex relationships between users and items [9]. However, these prior works only focused on a user and a target item without considering the user's previously consumed items, some of which may be related to the target item. While some prior works [14, 17] largely premised on unordered user interactions, users' interests are intrinsically dynamic and evolving. Based on the observation, [5, 11, 15, 30, 32] followed two paradigms to capture a user's sequential pattern: (i) *short-term* item-item transitions, or (ii) *long-term* item-item transitions.

However, user's interests can be highly diverse, so modeling only either *short-term* or *long-term* user intent does not fully capture the user's preferences, producing less effective recommendation results. To illustrate the point, we conducted an empirical analysis on *Amazon Video Games*, and *Toys and Games* datasets. First, we represent each item by a multi-hot encoding, where item j is represented by a vector $t \in \mathbb{R}^m$, position $i = 1$ if user i consumed the current item, and m denotes the total number of users in a dataset. For each user, her consumed items are sorted in the chronological order. Then, we calculated a cosine similarity score between each item and each of its previously consumed items. Then we selected the largest cosine similarity score per item per user. Figure 1 presents the density distribution of the consumed time interval (*x-axis*) between each pair of item and its most similar previously consumed item. We observe that there exists a bimodal distribution, where one (*left*) peak lays at a relative short-term period and the other (*right*) peak locates in a long-term period. The observation confirms that both long-term and short-term preferences played important roles on the user's

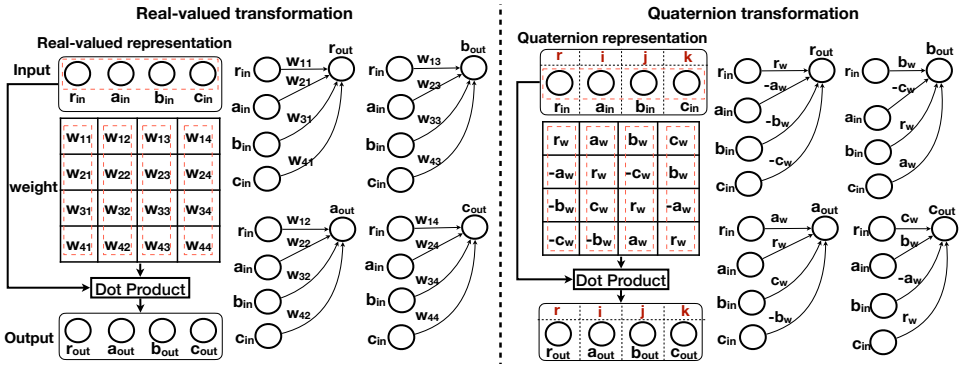

Figure 2: Comparison between real-valued transformation (Left) and Quaternion transformation (Right). We replace Hamilton product in Quaternion space with an equivalent dot product in real space for an easy reference.

current purchasing intent. We observe the same phenomenon from the other four datasets described in Section 6.

Based on the observation, we propose a Quaternion-based neural recommender system that models both long-term and short-term user preferences. Unlike the prior works [42, 46] which rely on Euclidean space, our proposed recommender system models both user's long-term and short-term preferences in a hypercomplex system (i.e., Quaternion Space) to further improve the recommendation quality. Concretely, we utilize Quaternion representations for all users, items and neural transformations in our proposed models. There are numerous benefits of the Quaternion utilization over the traditional real-valued representations in Euclidean space: (1) Quaternion numbers/vectors consist of a real component and three imaginary components (i.e. $\boldsymbol{i}, \boldsymbol{j}, \boldsymbol{k}$), encouraging a richer extent of expressiveness; (2) instead of using dot product in Euclidean space, Quaternion numbers/vectors operate on Hamilton product, which matches across multiple (inter-latent) Quaternion components and strengthens their inter-latent interactions, leading to a higher expressive model; (3) the weight sharing nature of Hamilton product leads to a model with a smaller number of parameters.

To illustrate these benefits of the Quaternion utilization, we show a comparison of a transformation process with Quaternion representations *vs.* real-valued representations in Figure 2. In Euclidean space, different output dimensions are produced by multiplying the same input with different weights. Given a real-valued 4-dimensional vector $[r_{in}, a_{in}, b_{in}, c_{in}]$, it takes a total of 16 parameters (i.e. 16 degrees of freedom) to transform into $[r_{out}, a_{out}, b_{out}, c_{out}]$. For Quaternion transformation, the input vector now is represented with 4 components, where r_{in} is the value of the real component, a_{in}, b_{in}, c_{in} are the corresponding values of the three imaginary parts $\boldsymbol{i}$, $\boldsymbol{j}$, $\boldsymbol{k}$. Due to the weight sharing nature of Hamilton product (refer to the Equa (3) in Section 4), different output dimensions take different combinations of the same input with only 4 weighting parameters $\{r_w, a_w, b_w, c_w\}$. The Quaternions provide a better inter-dependencies interaction coding and reduce 75% of the number of parameters compared with real-valued representations in Euclidean space (e.g., 4 unique parameters vs. 16 parameters).

To our best of knowledge, we are the first work that fully utilizes Quaternion space in modeling both user's long-term and short term interests. Furthermore, to increase our model's robustness, we propose a Quaternion-based Adversarial attack on Bayesian Personalized Ranking (QABPR) loss. As far as we know, we are the first, applying adversarial attack on Quaternion representations in the recommendation domain.

We summarize our contributions in the paper as follows:

- We propose novel Quaternion based models to learn a user's long-term and short-term interests more effectively. As a part of our framework, we propose Quaternion self-attention that works in Quaternion space.
- We propose a Quaternion-based Adversarial attack on BPR-loss to further improve the robustness of our model.
- We conduct extensive experiments to demonstrate the effectiveness of our models against 11 strong state-of-the-art baselines on six real-world datasets.

2 RELATED WORK

General Recommenders. Matrix Factorization is the most popular method to encode global user representations by using unordered user-item interactions [13, 18, 43]. Its basic idea is to represent users and items by latent factors and use dot product to learn the user-item affinity. Despite their success, they cannot model non-linear user-item relationships due to the linear nature of dot product. To overcome the limitation, neural network based recommenders were recently introduced [1, 9, 36, 38]. [9] combined a *generalized matrix factorization* component and a non-linear user-item interactions via a MLP architecture. [21, 24, 25] substituted the MLP architecture with the auto-encoder design. [35, 41] used memory augmentation to learn different user-item latent relationship. When non-existed users come with some observed interactions (i.e., recently created user accounts with some item interactions), the recommenders need to be rebuilt to generate their representations. To avoid these issues, current works encode users by combining the users' consumed item embeddings in two main streams: (i) taking average of the consumed items' latent representations [14, 17], or (ii) attentively summing [8] the consumed items' embeddings.

Despite their success, general recommenders mostly consider all users' unordered consumed items, and produce global/long-term user representations, which are supposed to be static, or changed slowly. Thus, they failed to capture the user's dynamic behavior, that is captured by the user's short-term preference (see Figure 1).

Sequential Recommenders. Sequential recommendation is known for its superiority to capture temporal dependencies between historical items [23]. Early works relied on Markov Chains to capture

item-item sequential patterns [2, 5, 30]. Other works exploited the convolution architecture to capture more complex temporal dependencies [32]. These methods used short-term item dependencies to model a user's dynamic interest. Other sequential recommenders focused on modeling long-term user preferences using RNN-based architectures [11, 20, 22, 40]. However, modeling either long-term user interests or short-term user interests is suboptimal since they concurrently affect a user's intent (Figure 1). Recent works combined both long and short-term user preferences in real-valued representations to obtain satisfactory results [15, 42, 46].

Compared with the prior works which used real-valued representations , we propose Quaternion-based models to capture the user's long-term and short-term interests. Quaternion was first introduced by [4] and it has recently shown its effectiveness over real-valued representations in NLP and computer vision domains [3, 27, 33, 47]. We acknowledge that *QCF* model [44] is the first Quaternion-based recommender. However, the authors used it as a simple extension of the matrix factorization method, where users and items are Quaternion embeddings. Thus, the benefits of Quaternion representation were not fully exploited in their network. Furthermore, they designed the model for a general recommendation problem, which has an inherent limitation of only modeling the user's global interest.

3 PROBLEM DEFINITION

Denote U=$\{u_1, u_2, ..., u_m\}$ as a set of all users where $m = |U|$ is the total number of users, and P=$\{p_1, p_2, ..., p_n\}$ as a set of all items where $n = |P|$ is the total number of items. Bold versions of those variables, which we will introduce in the following sections, indicate their respective latent representations/embeddings. Each user $u_i \in U$ consumes items in P, denoted by a chronological list $T^{(u_i)}$. We denote $L^{(u_i)}$ as the chronological list of long-term consumed items of u_i, and $S^{(u_i)}$ as the chronological list of short-term consumed items of u_i (i.e. s most recently consumed items in chronological order of the user u_i), $L^{u_i} \cup S^{u_i} = T^{(u_i)}$. Note that bold versions of $\boldsymbol{i}, \boldsymbol{j}, \boldsymbol{k}$ are used to indicate the three imaginary parts of a Quaternion, while their subscript versions are used as indices.

In this work, we propose and build Quaternion-based recommender systems by using both long-term and short-term user interests, denoted as $P(p_j|L^{(u_i)}, S^{(u_i)})$. Under an assumption that $L^{(u_i)}$ and $S^{(u_i)}$ are independent given the target item p_j, we model $P(p_j|L^{(u_i)}, S^{(u_i)})$ by modeling the user's long-term interest $P(p_j|L^{(u_i)})$ and short-term interest $P(p_j|S^{(u_i)})$ separately by using two different Quaternion-based neural networks. Then, we automatically fuse the two models to build a more effective recommender system.

4 PRELIMINARY ON QUATERNION

In this section, we cover important background on Quaternion Algebra and Quaternion Operators that we use to design our models.

Quaternion number: In mathematics, Quaternions are a hypercomplex number system. A Quaternion number X in a Quaternion space $\mathbb{H}$ is formed by a real component (r) and three imaginary components as follows:

$$X = r + a\boldsymbol{i} + b\boldsymbol{j} + c\boldsymbol{k}, \tag{1}$$

where $\boldsymbol{ijk} = \boldsymbol{i}^2 = \boldsymbol{j}^2 = \boldsymbol{k}^2 = -1$. The non-commutative multiplication rules of quaternion numbers are: $\boldsymbol{ij} = \boldsymbol{k}$, $\boldsymbol{jk} = \boldsymbol{i}$, $\boldsymbol{ki} = \boldsymbol{j}$, $\boldsymbol{ji} = -\boldsymbol{k}$, $\boldsymbol{kj} = -\boldsymbol{i}$, $\boldsymbol{ik} = -\boldsymbol{j}$. In Equa (1), r, a, b, c are real numbers $\in \mathbb{R}$. Note that we can extend r, a, b, c to real-valued vectors to obtain a Quaternion embedding, which we use to represent each user/item's latent features and conduct neural transformations. Operations on Quaternion embeddings are similar to Quaternion numbers.

Component-wise Quaternion Operators: Let f define an algebraic operator in real space $\mathbb{R}$. The *component-wise Quaternion operator* f on two Quaternions $X, Y \in \mathbb{H}$ is defined as:

$$f(X, Y) = f(r_X, r_Y) + f(a_X, a_Y)\boldsymbol{i} + f(b_X, b_Y)\boldsymbol{j} + f(c_X, c_Y)\boldsymbol{k} \tag{2}$$

For instance, if f is an *addition* operator (i.e. $f(a, b) = a + b$), then $f(X, Y)$ returns a component-wise Quaternion addition between X and Y. If f is a *dot product* operator (i.e. $f(a, b) = a^T b$), then $f(X, Y)$ returns a component-wise Quaternion *dot product* between X and Y. A similar description is applied when f is either *subtraction*, *scalar multiplication*, *product*, *softmax*, or *concatenate* operator, *.etc.*

Hamilton Product: The Hamilton product (denoted by the $\otimes$ symbol) of two Quaternions $X \in \mathbb{H}$ and $Y \in \mathbb{H}$ is defined as:

$$\begin{aligned} X \otimes Y =& (r_X r_Y - a_X a_Y - b_X b_Y - c_X c_Y) + \\ & (r_X a_Y + a_X r_Y + b_X c_Y - c_X b_Y)\boldsymbol{i} + \\ & (r_X b_Y - a_X c_Y + b_X r_Y + c_X a_Y)\boldsymbol{j} + \\ & (r_X c_Y + a_X b_Y - b_X a_Y + c_X r_Y)\boldsymbol{k} \end{aligned} \tag{3}$$

Activation function on Quaternions: Similar to [3, 28], we use a *split activation function* because of its stability and simplicity. *Split activation function* β on a Quaternion X is defined as:

$$\beta(X) = \alpha(r) + \alpha(a)\boldsymbol{i} + \alpha(b)\boldsymbol{j} + \alpha(c)\boldsymbol{k} \tag{4}$$

, where α is any standard activation function for real values.

Concatenate four components of a Quaternion: concatenates all four Quaternion components into one real-valued vector:

$$[X] = [r_X, a_X, b_X, c_X] \tag{5}$$

5 OUR PROPOSED MODELS

Figure 3 shows an overview of our proposals. First, our QUaternion-based self-Attentive Long term user Encoding (*QUALE*) learns a user's long-term interest by using long-term consumed items and the target item. Second, our QUaternion-based self-Attentive Short term user Encoding (*QUASE*) encodes the user's short-term intent by using short-term consumed items and the target item. Then our QUaternion-based self-Attentive Long Short term user Encoding (*QUALSE*) fuses both of the user preferences by using a Quaternion-based gating layer. We describe each component as follows:

5.1 QUaternion-based self-Attentive Long term user encoding (our QUALE model)

The most widely used technique for modeling the user long-term interests is the Asymmetric-SVD (ASVD) [17] model. Its basic idea is to encode each user and item by latent representations where the user representation is encoded by summing latent representations of the user's interacted items. To an extent, we propose a QUaternion-based self-Attentive Long term user Encoding (*QUALE*). *QUALE* represents each user and each item as Quaternion embeddings. Then, we encode each user by attentively summing Quaternion embeddings of her interacted items as follows:

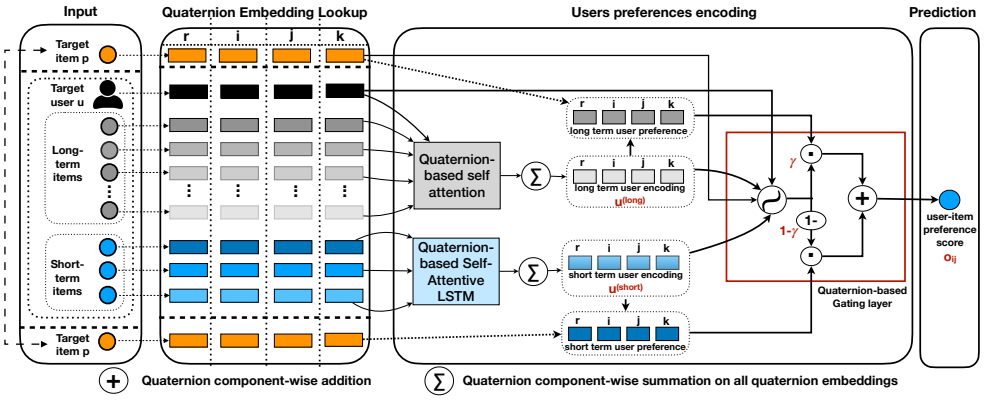

Figure 3: Our proposed architecture for modeling both long and short-term user interests using Quaternion representations.

$$\boldsymbol{u}_i^{(long)} = \sum_{k=1}^{|L^{(u_i)}|} \alpha_k \times \boldsymbol{p}_k^{(long)} \tag{6}$$

where $\boldsymbol{u}_i^{(long)}, \boldsymbol{p}_k^{(long)} \in \mathbb{H}$. The summation "$\sum$" and the multiplication "$\times$" are Quaternion component-wise operators, which are calculated by using Equa (2). We use our proposed Quaternion personalized self-attention mechanism to assign attentive scores $\alpha_k \in \mathbb{H}$ for different long-term items p_k.

Our *QUALE* model has four layers: Input, Quaternion Embedding, Encoding, and Output layers. We detail each layer as follows:

5.1.1 Input. *QUALE* requires a target user u_i, a target item p_j, and the user's list of l long-term items $L^{(u_i)}$ with $|L^{(u_i)}| = l$. l could be simply set to the maximum number of long-term items among all the users in a dataset. However, we observed that only several users in our datasets consumed an extremely large number of items compared to the majority of users. Hence, we set l to the upper bound of the boxplot approach (i.e. Q3 + 1.5IQR, where Q3 is the *third quartile*, and IQR is the *Interquartile range* of the sequence length distribution of all users). If a user has consumed less than l items, we pad the list with *zeroes* until its length reaches l.

5.1.2 Quaternion Embedding layer. It holds two Quaternion embedding matrices: a user context Quaternion embedding matrix $\mathcal{U}^{(long)} \in \mathbb{H}^{m \times d}$, and an item Quaternion embedding matrix $\mathcal{P}^{(long)} \in \mathbb{H}^{n \times d}$. Here, m and n are the respective number of users and items in the system. d is the Quaternion embedding size, and is measured by the total size of real-valued vectors of four Quaternion components ($d = |r| + |a| + |b| + |c|$, and $|r| = |a| = |b| = |c| = d/4$). By passing the target user u_i, the target item p_j, and long-term items p_k in the *Input* layer through the two respective Quaternion embedding matrices, we obtain the corresponding user context Quaternion embedding $\boldsymbol{q}_i^{(long)}$, target item Quaternion embedding $\boldsymbol{p}_j^{(long)}$ and long-term item Quaternion embeddings $\boldsymbol{p}_k^{(long)}$.

5.1.3 Encoding layer. Its main goal is to compute attentive scores for l Quaternion item embeddings in Equa (6). To do so, we propose a Quaternion personalized self-attention mechanism as follows:

We first compute the Hamilton product between each long-term item Quaternion embedding $\boldsymbol{p}_k^{(long)}$ ($k = \overline{1,l}$) and the Quaternion context embedding $\boldsymbol{q}_i^{(long)}$ of the target user u_i. Next, we use Equa (2) to multiply the results with the scaling factor $1/\sqrt{d}$ to eliminate the scaling effects. Then, we apply Component-wise Softmax (Equa (2)) to obtain Quaternion attention scores as follows:

$$\begin{bmatrix} \alpha_1 \\ \alpha_2 \\ \dots \\ \alpha_l \end{bmatrix} = \text{ComponentSoftmax}\left(\begin{bmatrix} \boldsymbol{p}_1^{(long)} \otimes \boldsymbol{q}_i^{(long)}/\sqrt{d} \\ \boldsymbol{p}_2^{(long)} \otimes \boldsymbol{q}_i^{(long)}/\sqrt{d} \\ \dots \\ \boldsymbol{p}_l^{(long)} \otimes \boldsymbol{q}_i^{(long)}/\sqrt{d} \end{bmatrix} \right) \tag{7}$$

.

To obtain the attentive long-term user encoding $\boldsymbol{u}_i^{(long)}$ of the user u_i, we first perform the component-wise product between the attention scores $[\alpha_1, \alpha_2, ..., \alpha_l]$ obtained in Equa (7) with its corresponding item Quaternion embeddings $[p_1^{(long)}, p_2^{(long)}, ..., p_l^{(long)}]$. Then we sum them up to obtain $\boldsymbol{u}_i^{(long)}$ as follows:

$$\boldsymbol{u}_i^{(long)} = \sum_{k=1}^{l} \alpha_k \times \boldsymbol{p}_k^{(long)} \tag{8}$$

Our proposed Quaternion personalized self-attention mechanism vs. the existing self-attention mechanism: Our proposed Quaternion personalized self-attention mechanism is different from the self-attention mechanism that has been widely used in the NLP tasks in two aspects. First, unlike the prior work [45], which uses a single global context to assign attentive scores for different dialogue states, our attention mechanism provides personalized contexts for different users. In the recommendation domain, the long-term/general user interests are supposed to be changed slowly, but user interests are various across users. In other words, a user's long-term context is quite static, but different from another user. Hence, using personalized contexts for different users is better than using a single global context, which is not personalized. Second, our attention mechanism adopts Hamilton product and works for Quaternion embeddings as input, instead of the real-valued embeddings like traditional self-attention mechanisms.

5.1.4 Output. We produce a long-term preference score $o_{ij}^{(long)}$ between the target user u_i and the target item p_j by computing the Component-wise dot product between the user long-term Quaternion encoding $\boldsymbol{u}_i^{(long)}$ obtained in Equa (8) and the target item Quaternion embedding $\boldsymbol{p}_j^{(long)}$. This results in a Quaternion score .

To obtain a real-valued scalar preference score used in the parameter estimation phase, we compute the average of the scalar values of four Quaternion components by following [44]:

$$o_{ij}^{(\text{long})} = \text{Average}(\text{ComponentDot}(\boldsymbol{u}_i^{(long)}, \boldsymbol{p}_j^{(long)})) \quad (9)$$

5.2 QUaternion-based self-Attentive Short term user Encoding (our QUASE model)

RNN-based models have gained a lot of attention because of their capability to capture item-to-item relationships [26, 40, 46]. However, due to its limitation in modeling a long sequence, we only exploit the RNN architecture to encode a user's short-term interest. Recently, [28] has introduced a Quaternion LSTM (QLSTM) model and has shown its efficiency and effectiveness over a traditional real-valued LSTM model. However, QLSTM used only the last hidden state as a latent summary of the input, which is suboptimal. To an extent, we propose a Quaternion-based self-Attentive LSTM model to learn a user's short-term interest. We name our proposal as a QUaternion-based self-Attentive Short term user Encoding (QUASE). *QUASE* has 4 layers: Input, Quaternion Embedding, Encoding, and Output layers. We describe each layer as follows:

5.2.1 Input. A target item p_j, and the chronological list of s short-term consumed items $S^{(u_i)}$ of the target user u_i with $|S^{(u_i)}| = s$, where s represents the maximum number of short-term items among all the users in a dataset. If a user has consumed less than s items, we pad the list with *zeroes* until its length reaches s.

5.2.2 Quaternion Embedding layer. It holds an item Quaternion Embedding matrix $\mathcal{P}^{(short)} \in \mathbb{H}^{n \times d}$. By passing the target item p_j, and s short-term items in the $S^{(u_i)}$ of the target user u_i through P^{short}, we obtain their corresponding Quaternion embeddings $\boldsymbol{p}_j^{(short)}$, and $\{\boldsymbol{p}_1^{(short)}, \boldsymbol{p}_2^{(short)}, ..., \boldsymbol{p}_s^{(short)}\}$.

5.2.3 Encoding layer. In this layer, we adapt the recently introduced Quaternion-based LSTM to model the item-item sequential transition. Denote $\boldsymbol{p}_t^{(short)}$ is the Quaternion embedding of the t^{th} short-term item $p_t \in S^{(u_i)}$ ($t = \overline{1,s}$). Let f_t, i_t, o_t, c_t, and h_t be the forget gate, input gate, output gate, cell state, and the hidden state of a Quaternion LSTM cell at time step t, respectively. We compute these variables as follows:

$$\begin{aligned}
f_t &= \sigma(W_f \otimes \boldsymbol{p}_t^{(short)} + R_f \otimes \boldsymbol{h_{t-1}} + g_f) \\
i_t &= \sigma(W_i \otimes \boldsymbol{p}_t^{(short)} + R_i \otimes \boldsymbol{h_{t-1}} + g_i) \\
o_t &= \sigma(W_o \otimes \boldsymbol{p}_t^{(short)} + R_o \otimes \boldsymbol{h_{t-1}} + g_o) \\
c_t &= f_t \times c_{t-1} + i_t \times \tanh(W_c \otimes \boldsymbol{p}_t^{(short)} + R_c \otimes \boldsymbol{h_{t-1}} + g_c) \\
h_t &= o_t \times tanh(c_t)
\end{aligned} \quad (10)$$

, where $W_f, R_f, W_i, R_i, W_o, R_o, W_c, R_c$ are Quaternion weight matrices. g_f, g_i, g_o, g_c are Quaternion bias vectors. f_t, i_t, o_t, c_t, h_t are Quaternion vectors. The "$\times$" sign denotes a component-wise *product* operator, which is calculated using Equa (2). *sigmoid* σ and *tanh* are split activation functions and are computed using the Equa (4).

Using Equa (10), given s short-term consumed items $p_1, p_2, ..., p_s$, we obtain their respective output Quaternion hidden states $\boldsymbol{h_1}, \boldsymbol{h_2}$, ..., $\boldsymbol{h_s}$. Then, we propose a Quaternion self-attention mechanism to combine all s output Quaternion hidden states before using it to predict the next item. Different from the long-term user preferences where they are supposed to be static or changed very slowly, the short-term user interests are dynamic and changed quickly. Hence, using a static user context for each user to make personalized attention like what we did for the *QUALE* model is not ideal. Instead, we define a Quaternion global context vector to capture the sequential transition patterns from item to item among all the users. Denote q as a Quaternion global context vector, the Quaternion-based self-attention score of each hidden state h_t is measured by:

$$\begin{bmatrix} \alpha_1^{(short)} \\ \alpha_2^{(short)} \\ \dots \\ \alpha_s^{(short)} \end{bmatrix} = \text{ComponentSoftmax}\left(\begin{bmatrix} \boldsymbol{h_1} \otimes \boldsymbol{q}/\sqrt{d} \\ \boldsymbol{h_2} \otimes \boldsymbol{q}/\sqrt{d} \\ \dots \\ \boldsymbol{h_t} \otimes \boldsymbol{q}/\sqrt{d} \end{bmatrix} \right) \quad (11)$$

, where $\alpha_1^{(short)}, \alpha_2^{(short)}, ..., \alpha_s^{(short)}$ are Quaternion numbers. To achieve the final short-term user Quaternion encoding, we perform a component-wise product between the Quaternion hidden states and their respective Quaternion attention scores, followed by a Hamilton product with a Quaternion weight matrix W and the split activation function *tanh*:

$$\boldsymbol{u}_i^{(short)} = tanh\left(W \otimes \left(\sum_{t=1}^{s} \alpha_t^{(short)} \times \boldsymbol{h_t} \right)\right) \quad (12)$$

Note that we also designed a Quaternion self-Attentive GRU , but its performance was slightly worse than the Quaternion self-Attentive LSTM (see Table 2 in Section 6). Thus, we only described the Quaternion self-Attentive LSTM due to space limitation.

5.2.4 Output. Similar to Equa (9), we produce the user u_i short-term preference score $o_{ij}^{(short)}$ over the target item p_j as follows:

$$o_{ij}^{(short)} = Average\big(ComponentDot(\boldsymbol{u}_i^{(short)}, \boldsymbol{p}_j^{(short)})\big) \quad (13)$$

5.3 QUaternion-based self-Attentive Long Short term user Encoding (QUALSE): a Fusion of QUASE and QUALE models

In this part, we aim to combine both user's long-term and short-term preferences modeling parts into one model, namely *QUALSE*, fusing *QUALE* and *QUASE* models. Inspired by the gated mechanism in LSTM [12] to balance the contribution of the current input and the previous hidden state, we propose a *personalized* Quaternion gated mechanism to fuse the long-term and short-term user interests learned in *QUALE* and *QUASE* models. Our *personalized* gating proposal is different to the traditional gating mechanism in two folds. First, gating weights in our proposal are in Quaternion space and the transformations are computed using the Hamilton product. Second, as users' behaviors differ from a user to another user, we additionally input the target user embeddings $\boldsymbol{u_i}$ to let the gating layer assign personalized scores for different users. The long-term and short-term interest fusion is computed as follows:

$$\begin{aligned}
\gamma_{ij}^{(long)} &= \sigma\big(W_g^{(1)} \otimes [\boldsymbol{u}_i^{(long)}, \boldsymbol{u}_i^{(short)}] + W_g^{(2)} \otimes \boldsymbol{u_i} + W_g^{(3)} \otimes \boldsymbol{p}_j\big) \\
o_{ij} &= W_o^{(1)}\big[\gamma_{ij}^{(long)} \times (\boldsymbol{u}_i^{(long)} \times \boldsymbol{p}_j^{(long)})\big] + \\
&\quad W_o^{(2)}\big[(1 - \gamma_{ij}^{(long)}) \times (\boldsymbol{u}_i^{(short)} \times \boldsymbol{p}_j^{(short)})\big]
\end{aligned} \quad (14)$$

, where $W_g^{(1)}$, $W_g^{(2)}$, and $W_g^{(3)}$ are Quaternion weight matrices, $\boldsymbol{u}_i^{(long)}$ and $\boldsymbol{u}_i^{(short)}$ are the user's long-term Quaternion encoding and short-term Quaternion encoding obtained in Equa (8) and (12), respectively. $[\cdot\,,\cdot]$ is the component-wise concatenate (Equa (2)) of two input Quaternion vectors. To compute the long-term gate $\gamma_{ij}^{(long)}$, $\boldsymbol{u_i}$ and $\boldsymbol{p_j}$ are introduced as an additional user context Quaternion embedding and a target item context Quaternion embedding to let the model know which long-term or short-term interests are more relevant. To measure the final output o_{ij}, since $\gamma_{ij}^{(long)}$ is a Quaternion vector while $o_{ij}^{(long)}$ and $o_{ij}^{(short)}$ are scalar values, we reconstruct the user's long-term interest by computing $\boldsymbol{u}_i^{(long)} \times \boldsymbol{p}_j^{(long)}$ and the short-term interest by measuring $\boldsymbol{u}_i^{(short)} \times \boldsymbol{p}_j^{(short)}$, which are also Quaternion vectors. Finally, to combine multiple dimensional features from the weighted long-term and short-term interest Quaternion vectors, we concatenate all their components, denoted by $[\cdot]$ (Equa (5)), and use two real-valued weight vectors $W_o^{(1)}$ and $W_o^{(2)}$ to produce a fused preference score as a scalar real number. Note that in *QUALSE*, *QUASE* and *QUALE* hold separated item memory to increase the their flexibility.

5.4 Parameter Estimation

5.4.1 Training with Bayesian Personalized Ranking (BPR) loss. Given a Quaternion matrix $E \in \mathbb{H}^{(m+n)\times d}$ as the Quaternion embeddings of all users and items in the system, and Θ as other parameters of the model, we aim to minimize the following BPR loss function:

$$\mathcal{L}_{BPR}(\mathcal{D}|E,\Theta) = \underset{E,\Theta}{\textbf{argmin}} \left(- \sum_{(i,j^+,j^-)} log\sigma(o_{ij^+} - o_{ij^-}) + \lambda_\Theta \|\Theta\|_2 + \lambda_E \|E\|_2 \right) \quad (15)$$

, where (i, j^+, j^-) is a triplet of a target user, a target item, and a negative item that is randomly sampled from the items set P. $\mathcal{D}$ denotes all the training instances. o_{ij^+} and o_{ij^-} are the respective positive and negative preference scores, that are computed by Equa (9), (13), (14), corresponding to *QUALE*, *QUASE* and *QUALSE* models. λ_Θ and λ_E are regularization hyper-parameters.

5.4.2 Training with Quaternion Adversarial attacks. Previous works have shown that neural networks are vulnerable to adversarial noise [7, 19]. Therefore, to increase the robustness of our models, we propose a Quaternion Adversarial attack on BPR loss, namely *QABPR*. *QABPR* inherits from traditional adversarial attacks for computer visions [19] and recommendation systems [7] but differs from them: *QABPR* applies for Quaternion space, while the formers apply for real-valued space. To our best of knowledge, ours is the first work using adversarial training on Quaternion space in the recommendation domain.

In *QABPR*, we first define learnable Quaternion perturbation noise δ on user and item Quaternion embeddings. Then, we perform the Quaternion component-wise addition (Equa (2)) to obtain crafted Quaternion embeddings. The learnable Quaternion noise δ is optimized such that the model mis-ranks between positive items and negative items (i.e. negative items have higher preference scores than positive items). Particularly, a *max* player learns

Table 1: Datasets' statistics with # of long-term items l.

Dataset	# of users	# of items	# of actions (density %)	l
Toys Games	36k	55k	251k (0.013%)	1,112
Cellphone Accessories	47k	45k	262k (0.012%)	109
Pet Supplies	25k	23k	160k (0.027%)	176
Video Games	24k	20k	196k (0.040%)	856
Apps for Android	79k	18k	555k (0.038%)	478
Yelp	22k	21k	481k (0.104%)	930

δ by maximizing the following cost function under the L_2 attack:

$$\mathcal{L}_{adv}(\mathcal{D}|E^* + \delta, \Theta^*) = \underset{\delta, \|\delta\|_2 \le \epsilon}{\textbf{argmax}} \left(- \sum_{(i,j^+,j^-)} log\sigma(o_{ij^+} - o_{ij^-}) + \lambda_\delta \|\delta\|_2 \right) \quad (16)$$

where ϵ is a noise magnitude hyper-parameter. E^* and Θ^* are optimal values of E and Θ that are pre-learned in Equa (15) and are fixed in Equa (16). $E^* + \delta$ is the crafted Quaternion embeddings. $\lambda_\Theta\|\Theta\|_2$ and $\lambda_E\|E\|_2$ in Equa (15) are ignored in Equa (16) as they become constant terms. $\lambda_\delta\|\delta\|_2$ is the noise regularization term.

Solving Equa (16) is expensive. Hence, we adopt the Fast Gradient Method [19] to approximate δ as follows:

$$\delta = \epsilon \frac{\nabla_\delta \mathcal{L}_{adv}(\mathcal{D}|E^*+\delta,\Theta^*)}{\|\nabla_\delta \mathcal{L}_{adv}(\mathcal{D}|E^*+\delta,\Theta^*)\|_2} \quad (17)$$

Then, a *min* player aims to minimize the following cost functions that incorporate both non-adversarial and adversarial examples:

$$\mathcal{L}_{QABPR}(\mathcal{D}|E, E+\delta^*, \Theta) = \underset{E,\Theta}{\textbf{argmin}} \left(\mathcal{L}_{BPR}(\mathcal{D}|E,\Theta) + \lambda_{adv}\mathcal{L}_{BPR}(\mathcal{D}|E+\delta^*,\Theta) \right) \quad (18)$$

where δ^* is the adversarial noise that is already learned in Equa (17), and is fixed in Equa (18). λ_{adv} is a hyper-parameter to balance the effect of the partial adversarial loss. Training *QABPR* now becomes playing a *minimax* game, where the *min* and *max* players play alternatively. We stop the game after a fixed number of epochs (i.e. 30 epochs) and report results based on the best *validation* performance.

Note that we name our *QUALE*, *QUASE*, and *QUALSE* trained with *QABPR* loss as *AQUALE*, *AQUASE*, and *AQUALSE* with "A" denotes "adversarial", respectively.

6 EMPIRICAL STUDY

In this section, we design experiments to answer the following research questions:

- **RQ1:** How do our proposals work compared to the baselines?
- **RQ2:** How do a user's long-term, short-term preference encoding models and the fused model perform?
- **RQ3:** Is using Quaternion representation helpful and why?
- **RQ4:** Are the gating fusion mechanism and the Quaternion BPR adversarial training helpful?

6.1 Datasets

We evaluate all models on **six** public benchmark datasets collected from two real world systems as follows:

- **Amazon datasets [6]**: As top-level product categories on Amazon are treated as independent datasets [15], we use 5 different Amazon category datasets to vary the sparsity, variability, and

Table 2: HIT@100 and NDCG@100 of all models. Best performances are in *bold*, best baseline's results are underlined. The last two lines show the relative improvement of QUALSE and AQUALSE compared to the best baseline's results.

	Methods	Toys Games		Cellphone Acc.		Pet Supplies		Video Games		Apps for Android		Yelp	
		HIT	NDCG	HIT	NDCG	HIT	NDCG	HIT	NDCG	HIT	NDCG	HIT	NDCG
(a)	AASVD	0.4343	0.1809	0.5640	0.2443	0.5523	0.2307	0.5503	0.2229	0.7149	0.3182	0.7212	0.3580
(b)	QCF	0.3869	0.1560	0.5514	0.2328	0.5319	0.2194	0.5217	0.1956	0.6638	0.2864	0.6774	0.3119
(c)	NeuMF++	0.3969	0.1553	0.5467	0.2291	0.5255	0.2174	0.4944	0.1934	0.6635	0.2791	0.6810	0.3208
(d)	NAIS	0.4331	0.1796	0.5648	0.2427	0.5569	0.2302	0.5587	0.2303	0.7076	0.3138	0.7277	0.3573
(e)	FPMC	0.3370	0.1335	0.4805	0.1970	0.4405	0.1812	0.5065	0.1980	0.6659	0.2847	0.6704	0.3204
(f)	AGRU	0.3747	0.1400	0.5211	0.2030	0.4690	0.1798	0.5337	0.1958	0.6969	0.2960	0.4722	0.1995
(g)	ALSTM	0.3886	0.1419	0.5159	0.2052	0.4630	0.1685	0.5156	0.1928	0.7043	0.2883	0.5644	0.2519
(h)	Caser	0.3889	0.1507	0.5747	0.2289	0.4786	0.1859	0.5502	0.1967	0.7098	0.3124	0.6718	0.3201
(i)	SASRec	0.4009	0.1545	0.5579	0.2239	0.5238	0.2124	0.5472	0.2107	0.6706	0.2781	0.7193	0.3381
(j)	SLi-Rec	0.4267	0.1823	0.5661	0.2387	0.5502	0.2311	0.5438	0.2276	0.7062	0.3117	0.7201	0.3516
(k)	ALSTM+AASVD	0.4394	0.1864	0.5701	0.2475	0.5542	0.2326	0.5502	0.2328	0.7173	0.3207	0.7222	0.3594
Our proposals													
	QUALE	0.4696	0.1997	0.6042	0.2685	0.5826	0.2483	0.5981	0.2503	0.7281	0.3248	0.7391	0.3723
	QUASE (GRU)	0.4080	0.1632	0.5612	0.5807	0.2438	0.5413	0.2246	0.2207	0.7198	0.3223	0.6917	0.3324
	QUASE (LSTM)	0.4095	0.1664	0.5844	0.2475	0.5453	0.2263	0.5591	0.2261	0.7300	0.3300	0.6929	0.3311
	QUALSE	**0.4760**	**0.2043**	**0.6127**	**0.2777**	**0.5913**	**0.2539**	**0.6018**	**0.2551**	**0.7373**	**0.3364**	**0.7442**	**0.3781**
	AQUALE	0.4831	0.2055	0.6105	0.2748	0.5902	0.2553	0.6045	0.2593	0.7346	0.3306	0.7440	0.3786
	AQUASE (LSTM)	0.4495	0.1847	0.6056	0.2572	0.5520	0.2329	0.5762	0.2351	0.7285	0.3292	0.7048	0.3450
	AQUALSE	**0.4921**	**0.2098**	**0.6204**	**0.2842**	**0.6011**	**0.2612**	**0.6137**	**0.2605**	**0.7477**	**0.3440**	**0.7448**	**0.3814**
Imprv. of QUALSE		**+8.33%**	**+9.60%**	**+6.61%**	**+12.20%**	**+6.18%**	**+9.16%**	**+7.71%**	**+9.58%**	**+2.79%**	**+4.90%**	**+2.27%**	**+5.20%**
Imprv. of AQUALSE		**+11.99%**	**+12.55%**	**+7.95%**	**+14.83%**	**+7.94%**	**+12.30%**	**+9.84%**	**+11.90%**	**+4.24%**	**+7.27%**	**+2.35%**	**+6.12%**

data size: *Apps for Android*, *Cellphone Accessories*, *Pet Supplies*, *Toys and Games*, and *Video Games*.

- **Yelp dataset**: This is a user rating dataset on businesses. We use the dataset obtained from [10].

For data preprocessing, we adopted a popular *k-core* preprocessing step [6] (with k=5), filtering out users and items with less than 5 interactions. All observed ratings are considered as positive interactions and the remaining as negative interactions. The maximum number of short-term items is set to $s = 5$ in all datasets as it covers the short-term peak (see Figure 1). Table 1 summarizes the statistics of all datasets, as well as their number of long-term items l.

6.2 State-of-the-art Baselines

We compared our proposed models with **11** strong state-of-the-art recommendation models as follows:

- **AASVD**: It is an attentive version of the well-known Asymmetric SVD model (ASVD) [17], where real-valued self-attention is applied to measure attentive contribution of previously consumed items by a user.
- **QCF** [44]: It is a state-of-the-art recommender that represents users/items by Quaternion embeddings.
- **NeuMF++** [9]: It models non-linear user-item interactions by using a MLP and a Generalized MF (GMF) component. We pretrained MLP and GMF to obtain NeuMF's best performance.
- **NAIS** [8]: It is an extension of *ASVD* where contribution of consumed items to the target item is attentively assigned. We adopt $NAIS_{prod}$ version as it led to its best results.
- **FPMC** [30]: It is a state-of-the-art sequential recommender. It uses the first-order Markov to model the transition between the next item and the previously consumed items.
- **AGRU**: It is an extension of the well-known GRU4Rec [11], where we use an attention mechanism to combine different hidden states. We experiment with two attention mechanisms: real-valued self-attention, and real-valued *prod attention* proposed by [8]. Then we report its best performance.
- **ALSTM**: It is a LSTM based model. Similar to AGRU, we experiment with the real-valued self-attention and the *prod attention* [8], and then report its best results.
- **Caser** [32]: It embedded a sequence of recently consumed items into an "image" in time and latent spaces, and uses convolution neural network to learn sequential patterns as local features of an image using different horizontal and vertical filters.
- **SASRec** [15]: It is a strong sequential recommender model. It uses the self-attention mechanism with a multi-head design to identify relevant items for next predictive items.
- **Sli-Rec** [42]: It uses a time-aware controller to control the state transition. Then it uses an attention-based framework to fuse a user's long-term and short-term preferences.
- **ALSTM+AASVD**: It is our implementation that resembles the same architecture as our proposed Quaternion fusion approach, except that it uses Euclidean space instead of Quaternion space. The purpose of implementing and using it as a baseline is to present the effectiveness of our framework and Quaternion representations over the real-valued representations.

First four baselines (AASVD, QCF, NeuMF++, and NAIS) are classified as user's long-term interest encoding models. Next four baselines (FPMC, AGRU, ALSTM, and Caser) are user's short-term interest encoding models, and *SASRec, SLi-Rec, and ALSTM+AASVD* encode both user's long-term and short-term intents. Note that we performed an experiment with *DIEN* [46] (i.e. a long short-term

modeling baseline) based on the authors' public source code, which produced surprisingly low results, so we omit its detailed results. We also experimented with *ASVD*, LSTM, GRU and Quaternion LSTM but do not report their results due to space limitation and their worse results. Similarly, we omit *BPR* [29] and *FISM* [14] results due to their less impressive performance.

6.3 Experimental Settings

Protocol: We adopt a well-known and practical 70/10/20 splitting proportions to divide each dataset into train/validation (or development)/test sets [21, 34]. All user-item interactions are sorted in ascending order in terms of the interaction time. Then, the first 70% of all interactions are used for training, the next 10% of all interactions are used for development, and the rest is used for testing. We follow [39, 41] to sample 1,000 unobserved items that the target user has not interacted before, and rank all her positive items with these 1,000 unobserved items for testing models.

Evaluation metrics: We evaluate the performances of all models by using two well-known metrics: *Hit* Ratio (*HIT@N*), and Normalized Discounted Cumulative Gain (*NDCG@N*). *HIT@N* measures whether all the test items are in the recommended list or not, while *NDCG@N* takes into account the position of the test items, and assigns higher scores if test items are at top-rank positions.

Hyper-parameters Settings: All models are trained with *Adam* optimizer [16]. A learning rate is chosen from {0.001, 0.0005}, and regularization hyperparameters are chosen from {0, 0.1, 0.001, 0.0001}. An embedding size d is chosen from {32, 48, 64, 96, 128}. Note that for Quaternion embeddings, each component value is a vector of size $\frac{d}{4}$. The number of epochs is 30. The batch size is 256. The number of MLP layers in NeuMF++ is tuned from {1, 2, 3}. The number of negative samples per one positive instance is 4 for training models. The settings of *Caser*, *NAIS*, *SASRec* are followed by their reported default settings. In training with *QABPR* loss, the regularization λ_{adv} is set to 1. The noise magnitude ϵ is chosen from {0.5, 1, 2}. The adversarial noise is added only in training process, and is initialized as *zero*. All hyper-parameters are tuned by using the validation set.

6.4 Experimental Results

6.4.1 ***RQ1: Performance comparison.*** Table 2 shows that our proposed fused models *QUALSE* and *AQUALSE* outperformed all the compared baselines. On average, *QUALSE* improved *Hit@100* by 5.65% and *NDCG@100* by 8.44% compared to the best baseline's performances. *AQUALSE* gains additional improvement over *QUALSE*, enhancing *Hit@100* by 7.39% and *NDCG@100* by 10.83% on average compared to the best baseline. The improvement of our proposals over the baselines is significant under the Directional Wilcoxon signed-rank test (*p-value* < 0.015). We also observed similar results on all six datasets when we measure *Hit@1* and *NDCG@1*. In particular, our *QUALSE* improved *Hit@1* by 6.87% and *NDCG@1* by 8.71% on average compared with the best baseline. *AQUALSE* improved *Hit@1* by 8.43% and *NDCG@1* by 10.27% on average compared with the best baseline, confirming its consistent effectiveness.

6.4.2 Varying top-N recommendation list and embedding size: To further provide detailed effectiveness of our proposals, we compare QUALSE and AQUALSE models with the top-5 baselines when varying the embedding size from {32, 48, 64, 96, 128} and the *top-N* recommendation list from {10, 20, 50, 100}.

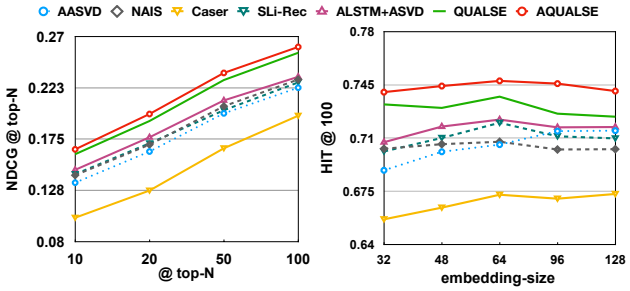

(a) NDCG@topN in Video Games **(b) HIT@100 in Yelp.**

Figure 4: Performance of our models and the top-5 baselines when varying a *top-N* recommendation list (left) and an embedding size (right).

Figure 4a shows that even with small *top-N* values (e.g., @10), our models consistently outperformed all the compared baselines in the *Video Games* dataset, improving the ranking performance by a large margin of 9.25%~12.30% on average. Specifically, at *top-N*=10 in *Video Games* dataset, QUALSE and AQUALSE improves NDCG@10 over the best baseline by 9.9% and 12.97%, respectively.

Figure 4b shows the HIT@100 performance of our QUALSE and AQUALSE models, and the top-5 baselines in the Yelp dataset when varying the embedding size. We observe that our proposals outperformed all the baselines. Interestingly, while non-adversarial models are more sensitive to the change of the embedding size, our adversarial AQUALSE model is relatively smoother when varying the embedding size. The result makes sense because the adversarial learning reduces the noise effect. Because of the space limitation, we only show detailed results of the *Video Games* and *Yelp* datasets.

6.4.3 ***RQ2: Effect of the long-term and short-term encoding components?*** Using reported results in Table 2, we first compare long-term encoding models (i.e. (a)-(d), and *QUALE*, *AQUALE*) with short-term encoding models (i.e. (e)-(h), and *QUASE*, *AQUASE*). In general, long-term encoding models work better than short-term encoding models. For instance, NAIS (i.e. best long-term encoding baseline) improves 8.5% on average on six datasets compared with Caser (i.e. best short-term encoding baseline). Similarly, our long-term encoding *QUALE* model works better than our short-term encoding *QUASE* model, enhancing 9.2% on average over six datasets. To investigate this phenomenon, we plot the density distribution of item-item similarity scores in test sets of two datasets *Pet-Supplies* and *Yelp* in Figure 5. We observe higher peaks on long-term item-item relationships in the curves, explaining why long-term encoding models work better than short-term encoding models.

Next, we compare the fused models with models that encode either long-term or short-term users preferences. Table 2 shows that models, which consider both user's long-term and short-term preferences, work better than other models, which encode either user's long-term or short-term interests. Both (j) and (k) baselines generally work better than (a)–(h) baselines. Specifically, our QUALSE and AQUALSE models improve 7.9%~10.0% on average over six datasets compared to the best baseline from (a)–(h). These observations show the effectiveness of modeling both user's long-term and short-term interests. Among models, which consider both user long-term and short-term interests, SASRec performed the worst compared to baselines (i)–(k) and our QUALSE and AQUALSE. This

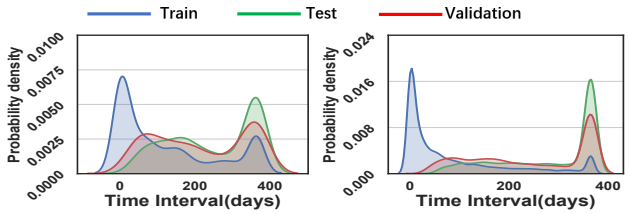

(a) Pet Supplies dataset. (b) Yelp dataset.

Figure 5: Density distribution of item-item similarity scores in train/vad/test sets of *Pet Supplies* and *Yelp* datasets.

is due to the fact that SASRec models user's long-term and short-term interests implicitly and concurrently by using the Transformer multi-head attention mechanism. But, SLi-Rec, ALSTM+AASVD, and our proposals model the two preferences explicitly and separately, and then combine them later on, increasing flexibility. Note that, although SLi-Rec employed a time-aware attentional LSTM to better model the user's short-term preferences, our ALSTM+AASVD implementation works slightly better than SLi-Rec due to its two distinct properties: (i) the personalized self-attention in AASVD, where each user is parameterized by her own context vector, and (ii) the personalized gating fusion.

6.4.4 ***RQ3: Is using Quaternion representation helpful?*** In Table 2, we compare different model pairs: *AASVD* vs. *QUALE*, *ALSTM* vs. *QUASE (LSTM)*, *AGRU* vs. *QUASE (GRU)*, and *ALSTM+AASVD* vs. *QUALSE*. Two methods under the same pair have similar architecture (again, *ALSTM+AASVD* was implemented by us, following our QUALSE architecture to show effectiveness of Quaternion representation). But, the first method of each pair uses real-valued representations and the second method of each pair uses Quaternion representations. Table 2 shows that *QUALE* works better than *AASVD*. In six datasets, on average, *QUALE* improves *Hit@100* by 5.60% and *NDCG@100* by 7.71% compared to *AASVD*. Similarly, we observe the same patterns from the other three model pairs. Moreover, when comparing our long-term encoding *QUALE* and *AQUALE* models with other long-term encoding baselines (a)-(e), our models outperformed the baselines, improving *HIT@100* by 5.16% and 6.55%, and enhancing *NDCG@100* by 7.11% and 9.83%, respectively. Similarly, our short-term encoding *QUASE* and *AQUASE* using LSTM also work better than other short-term encoding baselines (f)-(h), improving *HIT@100* by 4.75% and 8.09%, and enhancing *NDCG@100* by 10.57% and 15.33%, respectively. All of these results confirm the effectiveness of modeling user's interests by using Quaternion representations over Euclidean representations.

Why Quaternion representations help improve the performance? Since attention mechanism is the key success in deep neural networks [37], we analyze how our models assign attention weights compared to their respective real-valued models. We first measure the item-item Pointwise Mutual Information (PMI) scores (i.e. $PMI(j,t) = log\frac{P(j,t)}{P(j)\times P(t)}$) using the training set. The PMI score between two items (j,t) gives us the co-occurrence information between item j and item t, or how likely the target item j will be preferred by the target user when the item t is already in her consumed item list. We perform *softmax* on all item-item PMI scores. Then, we compare with the generated attention scores from our proposed models and ones from their respective real-valued baseline models.

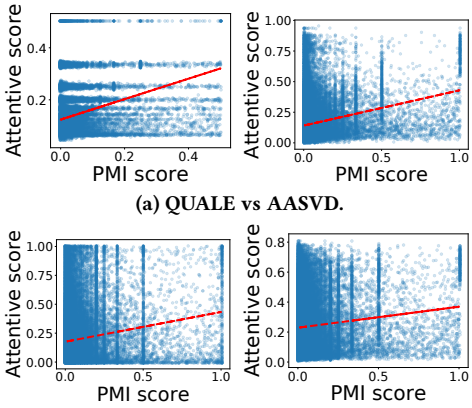

(a) QUALE vs AASVD.

(b) QUASE vs ALSTM.

Figure 6: Comparison of attention scores between (QUALE vs AASVD) and (QUASE vs ALSTM) in the Apps for Android dataset. Pearson correlation ρ between attention scores and PMI scores are: $\rho_{QUALE} = 0.232 > \rho_{AASVD} = 0.216$, and $\rho_{QUASE} = 0.148 > \rho_{ALSTM} = 0.1$.

Figure 6 shows the scatter plots and Pearson correlation comparison using the *Apps for Android* dataset. We see that *QUALE, QUASE* tend to correlate more positively with the PMI scores than their respective real-valued models *AASVD, ALSTM*. In another word, our Quaternion-based models assign higher scores for co-occurred item pairs. We reason coming from two aspects of Quaternion representations. First, Hamilton product in Quaternion space encourages strong inter-latent interactions across Quaternion components. Second, since our proposed self-attention mechanism produces scores in Quaternion space, the output attention scores have four values *w.r.t* four Quaternion components. This can be thought as similar to the multi-head attention mechanism [37] (but not exactly same because of the weight shared in Quaternion transformation), where the proposed attention mechanism learns to attend different aspects from the four Quaternion components. All of these explain why we got better results compared to the respective real-valued models.

6.4.5 ***RQ4: Effect of the personalized gated fusion and the QABPR loss?*** Table 2 shows that in real-valued representations, *ALSTM+ASVD* works better than *AASVD* and *ALSTM* in all six datasets. Similarly, in Quaternion representations, the fused *QUALSE* model generally works better than its two degenerated *QUALE* and *QUASE* models. In the six datasets, both *QUALSE* and *AQUALSE* perform better than their degenerated (adversarial) versions, improving 2% on average *w.r.t* both *HIT@100* and *NDCG@100*. The results confirm the effectiveness of fusing long-term and short-term user preferences in both of *QUALSE* and *AQUALSE*.

We further compare our gating fusion with a weight fixing method, where we vary a contribution score $c \in [0,1]$ for the user's short-term preference encoding part and $1-c$ for the long-term part. We see that the gating fusion improves 4.82% on average over six datasets compared to the weight fixing method, again confirming the effectiveness of our personalized gating fusion method.

Is Quaternion Adversarial training on BPR loss helpful? We compare our proposed models training with *BPR* loss (i.e. *QUALE, QUASE (LSTM)*, and *QUALSE* models) and our proposed models training with *QABPR* loss (i.e. *AQUALE, AQUASE (LSTM)*, and *AQUALSE*).

First, we observe that *AQUASE* boosted *QUASE* performance by a large margin: improving *HIT@100* by 3.2% and *NDCG@100* by 4.29% on average in the six datasets. *AQUALE* and *AQUALSE* also improve *QUALE* and *QUALSE* by 1.92% and 1.91% on average of both *HIT@100* and *NDCG@100* over six datasets, respectively. These results show the effectiveness of the adversarial attack on Quaternion representations with our *QABPR* loss.

7 CONCLUSION

In this paper, we have shown that user's short-term and long-term interests are complementary and both of them are indispensable. We fully utilized Quaternion space and proposed three novel Quaternion-based models: (1) a *QUALE* model learned the user's long-term intents, (2) a *QUASE* model learned the user's short-term interests, and (3) a *QUALSE* model fused *QUALE* and *QUASE* to learn both user's long-term and short-term preferences. We also proposed a Quaternion-based Adversarial attack on Bayesian Personalized Ranking (QABPR) loss to improve the robustness of our proposals. Through extensive experiments on six real-world datasets, we showed that our *QUALSE* improved 6.87% at *HIT@1* and 8.71% at *NDCG@1*, and *AQUALSE* improved 8.43% at *HIT@1* and 10.27% at *NDCG@1* on average compared with the best baseline. Our proposed models consistently achieved the best results when varying *top-N* (e.g., HIT@100 and NDCG@100). These results show the effectiveness of our proposed framework.

8 ACKNOWLEDGMENTS

This work was supported in part by NSF grant CNS-1755536, AWS Cloud Credits for Research, and Google Cloud.

REFERENCES

[1] Travis Ebesu, Bin Shen, and Yi Fang. 2018. Collaborative memory network for recommendation systems. In *SIGIR*. 515–524.
[2] Shanshan Feng, Xutao Li, Yifeng Zeng, Gao Cong, Yeow Meng Chee, and Quan Yuan. 2015. Personalized ranking metric embedding for next new POI recommendation. In *IJCAI*. 2069–2075.
[3] Chase J Gaudet and Anthony S Maida. 2018. Deep quaternion networks. In *IJCNN*. 1–8.
[4] William Rowan Hamilton. 1844. LXXVIII. On quaternions; or on a new system of imaginaries in Algebra: To the editors of the Philosophical Magazine and Journal. *The London, Edinburgh, and Dublin Philosophical Magazine and Journal of Science* 25, 169 (1844), 489–495.
[5] Ruining He, Wang-Cheng Kang, and Julian McAuley. 2017. Translation-based recommendation. In *RecSys*. 161–169.
[6] Ruining He and Julian McAuley. 2016. Ups and downs: Modeling the visual evolution of fashion trends with one-class collaborative filtering. In *WWW*. 507–517.
[7] Xiangnan He, Zhankui He, Xiaoyu Du, and Tat-Seng Chua. 2018. Adversarial personalized ranking for recommendation. In *SIGIR*. 355–364.
[8] Xiangnan He, Zhankui He, Jingkuan Song, Zhenguang Liu, Yu-Gang Jiang, and Tat-Seng Chua. 2018. NAIS: Neural attentive item similarity model for recommendation. *IEEE TKDE* 30, 12 (2018), 2354–2366.
[9] Xiangnan He, Lizi Liao, Hanwang Zhang, Liqiang Nie, Xia Hu, and Tat-Seng Chua. 2017. Neural collaborative filtering. In *WWW*. 173–182.
[10] Xiangnan He, Hanwang Zhang, Min-Yen Kan, and Tat-Seng Chua. 2016. Fast matrix factorization for online recommendation with implicit feedback. In *SIGIR*. 549–558.
[11] Balázs Hidasi, Alexandros Karatzoglou, Linas Baltrunas, and Domonkos Tikk. 2016. Session-based recommendations with recurrent neural networks. In *ICLR*.
[12] Sepp Hochreiter and Jürgen Schmidhuber. 1997. Long short-term memory. *Neural computation* 9, 8 (1997), 1735–1780.
[13] Yifan Hu, Yehuda Koren, and Chris Volinsky. 2008. Collaborative filtering for implicit feedback datasets. In *ICDM*. 263–272.
[14] Santosh Kabbur, Xia Ning, and George Karypis. 2013. Fism: factored item similarity models for top-n recommender systems. In *KDD*. 659–667.
[15] Wang-Cheng Kang and Julian McAuley. 2018. Self-attentive sequential recommendation. In *ICDM*. 197–206.
[16] Diederik P Kingma and Jimmy Ba. 2015. Adam: A method for stochastic optimization. In *ICLR*.
[17] Yehuda Koren. 2008. Factorization meets the neighborhood: a multifaceted collaborative filtering model. In *KDD*. 426–434.
[18] Yehuda Koren, Robert Bell, and Chris Volinsky. 2009. Matrix factorization techniques for recommender systems. *Computer* 42, 8 (2009), 30–37.
[19] Alexey Kurakin, Ian Goodfellow, and Samy Bengio. 2017. Adversarial examples in the physical world. *ICLR Workshop* (2017).
[20] Jing Li, Pengjie Ren, Zhumin Chen, Zhaochun Ren, Tao Lian, and Jun Ma. 2017. Neural attentive session-based recommendation. In *CIKM*. 1419–1428.
[21] Dawen Liang, Rahul G Krishnan, Matthew D Hoffman, and Tony Jebara. 2018. Variational autoencoders for collaborative filtering. In *WWW*. 689–698.
[22] Qiang Liu, Shu Wu, Diyi Wang, Zhaokang Li, and Liang Wang. 2016. Context-aware sequential recommendation. In *ICDM*. 1053–1058.
[23] Chen Ma, Peng Kang, and Xue Liu. 2019. Hierarchical gating networks for sequential recommendation. In *KDD*. 825–833.
[24] Chen Ma, Peng Kang, Bin Wu, Qinglong Wang, and Xue Liu. 2019. Gated attentive-autoencoder for content-aware recommendation. In *WSDM*. 519–527.
[25] Chen Ma, Yingxue Zhang, Qinglong Wang, and Xue Liu. 2018. Point-of-interest recommendation: Exploiting self-attentive autoencoders with neighbor-aware influence. In *CIKM*. 697–706.
[26] Shumpei Okura, Yukihiro Tagami, Shingo Ono, and Akira Tajima. 2017. Embedding-based news recommendation for millions of users. In *KDD*. 1933–1942.
[27] Titouan Parcollet, Mohamed Morchid, and Georges Linarès. 2019. Quaternion convolutional neural networks for heterogeneous image processing. In *ICASSP*. IEEE, 8514–8518.
[28] Titouan Parcollet, Mirco Ravanelli, Mohamed Morchid, Georges Linarès, Chiheb Trabelsi, Renato De Mori, and Yoshua Bengio. 2019. Quaternion recurrent neural networks. In *ICLR*.
[29] Steffen Rendle, Christoph Freudenthaler, Zeno Gantner, and Lars Schmidt-Thieme. 2009. BPR: Bayesian personalized ranking from implicit feedback. In *UAI*. 452–461.
[30] Steffen Rendle, Christoph Freudenthaler, and Lars Schmidt-Thieme. 2010. Factorizing personalized markov chains for next-basket recommendation. In *WWW*. 811–820.
[31] Paul Resnick and Hal R Varian. 1997. Recommender systems. *Commun. ACM* 40, 3 (1997), 56–58.
[32] Jiaxi Tang and Ke Wang. 2018. Personalized top-n sequential recommendation via convolutional sequence embedding. In *WSDM*. 565–573.
[33] Yi Tay, Aston Zhang, Luu Anh Tuan, Jinfeng Rao, Shuai Zhang, Shuohang Wang, Jie Fu, and Siu Cheung Hui. 2019. Lightweight and efficient neural natural language processing with quaternion networks. In *ACL*. 1494–1503.
[34] Thanh Tran, Kyumin Lee, Yiming Liao, and Dongwon Lee. 2018. Regularizing matrix factorization with user and item embeddings for recommendation. In *CIKM*. 687–696.
[35] Thanh Tran, Xinyue Liu, Kyumin Lee, and Xiangnan Kong. 2019. Signed Distance-based Deep Memory Recommender. In *WWW*. 1841–1852.
[36] Thanh Tran, Renee Sweeney, and Kyumin Lee. 2019. Adversarial mahalanobis distance-based attentive song recommender for automatic playlist continuation. In *SIGIR*. 245–254.
[37] Ashish Vaswani, Noam Shazeer, Niki Parmar, Jakob Uszkoreit, Llion Jones, Aidan N Gomez, Łukasz Kaiser, and Illia Polosukhin. 2017. Attention is all you need. In *NeurIPS*. 5998–6008.
[38] Lucas Vinh Tran, Tuan-Anh Nguyen Pham, Yi Tay, Yiding Liu, Gao Cong, and Xiaoli Li. 2019. Interact and decide: Medley of sub-attention networks for effective group recommendation. In *SIGIR*. 255–264.
[39] Xiang Wang, Xiangnan He, Meng Wang, Fuli Feng, and Tat-Seng Chua. 2019. Neural graph collaborative filtering. In *SIGIR*. 165–174.
[40] Chao-Yuan Wu, Amr Ahmed, Alex Beutel, Alexander J Smola, and How Jing. 2017. Recurrent recommender networks. In *WSDM*. 495–503.
[41] Xin Xin, Xiangnan He, Yongfeng Zhang, Yongdong Zhang, and Joemon Jose. 2019. Relational collaborative filtering: Modeling multiple item relations for recommendation. In *SIGIR*. 125–134.
[42] Zeping Yu, Jianxun Lian, Ahmad Mahmoody, Gongshen Liu, and Xing Xie. 2019. Adaptive user modeling with long and short-term preferences for personalized recommendation. In *IJCAI*. 4213–4219.
[43] Hanwang Zhang, Fumin Shen, Wei Liu, Xiangnan He, Huanbo Luan, and Tat-Seng Chua. 2016. Discrete collaborative filtering. In *SIGIR*. 325–334.
[44] Shuai Zhang, Lina Yao, Lucas Vinh Tran, Aston Zhang, and Yi Tay. 2019. Quaternion Collaborative Filtering for Recommendation. In *IJCAI*. 4313–4319.
[45] Victor Zhong, Caiming Xiong, and Richard Socher. 2018. Global-Locally Self-Attentive Encoder for Dialogue State Tracking. In *ACL*. 1458–1467.
[46] Guorui Zhou, Na Mou, Ying Fan, Qi Pi, Weijie Bian, Chang Zhou, Xiaoqiang Zhu, and Kun Gai. 2019. Deep interest evolution network for click-through rate prediction. In *AAAI*, Vol. 33. 5941–5948.
[47] Xuanyu Zhu, Yi Xu, Hongteng Xu, and Changjian Chen. 2018. Quaternion convolutional neural networks. In *ECCV*. 631–647.